Sensitivity of Seismic Site Response to Fluctuations in Water Levels

M. Mirshekari
Geosyntec Consultants, Acton, MA, USA

M. Ghayoomi
University of New Hampshire, Durham, NH, USA

J. Kaklamanos
Merrimack College, North Andover, MA USA

ABSTRACT: Differences in the degree of saturation in soil layers, from the time the soil properties were measured to the time an earthquake occurs, can influence seismic site response observations. To investigate the potential influence of variations in groundwater levels, equivalent linear analyses were performed whereby the groundwater table was changed and soil properties were subsequently adjusted for each scenario. Data from the Kiban-Kyoshin (KiK-net) network of surface-downhole seismometers were used as the baseline for the validation of numerical analyses. Surface-to-rock ratios of response spectra and Fourier transfer functions were numerically calculated for different groundwater level scenarios. Unsaturated soil conditions were modeled by increasing the suction and effective stress in the vadose zone. Stronger ground motion amplifications were observed when the groundwater water level was lowered. This trend is associated with simultaneous effects of shear modulus, damping, and unit weight on seismic response of soil profiles with different groundwater levels.

1 INTRODUCTION

Propagation of seismic waves through ground layers with different hydromechanical properties (i.e. shear modulus, damping, and soil-water retention curves) alters the amplitude, frequency content, and duration of earthquake motions. This influence of near-surface geologic materials on earthquake ground motions is commonly assessed through site response analyses. The effects of local site conditions and input motion characteristics on site response analyses have been addressed in numerous field monitoring, laboratory experiments, and numerical studies (e.g. Boore et al. 1994, Adalier and Elgamal 2001, Stewart et al. 2003, Kaklamanos and Bradley 2018). Partial saturation can lead to higher soil stiffness (Lu and Likos 2006, Jarast and Ghayoomi 2017). Differences in stiffness can alter dynamic soil properties (Mancuso et al. 2002, Hoyos et al. 2015, Ghayoomi et al. 2017, Mousavi and Ghayoomi 2018, Gheibi and Hedayat 2018) and, in turn, lead to variations in seismic site response (D'Onza et al. 2008, Mirshekari and Ghayoomi 2015, 2017a). The difference between the degree-of-saturation profiles in soil layers at the time when the shear wave velocity is measured (and implemented in site response models) and the time when the seismic event occurs could lead to variations in observations of seismic site response. These altered soil properties can introduce uncertainties in site response analysis and assessment, which have yet to be properly evaluated.

In this study, numerical analyses were performed using DEEPSOIL (Hashash et al. 2016) through an Equivalent-Linear (EL) approach. Data from surface-downhole station pairs, as part of the Kiban-Kyoshin network (KiK-net) database (Aoi et al. 2000), were used as the baseline ground motion data for validation and parametric evaluation. The depth of water table was changed from the baseline depth (inferred from the compression wave velocity profile at the site) and the influence of different material parameters (i.e. small-strain shear modulus, damping, modulus reduction factor, unit weight, and soil type) was evaluated. The impact of soil parameters, both individually and collectively, on Site Specific Response Analysis (SSRA) was investigated through inspecting the changes in surface-to-base Ratio of Response Spectra (RRS), their residual values, and Fast Fourier Transform (FFT) transfer functions.

2 METHODS

2.1 *Site Selection*

An instrumented site, suitable for 1-D site response analysis (Thompson et al. 2012), was selected from the suite of KiK-net sites. Station NMRH04, located in Nemuro sub-prefecture on eastern Hokkaido Island in Japan (Figure 1a), was chosen in this study because it contains fine sand close to the ground surface. The presence of finer materials allows for a clearer demonstration of the influence of partial saturation on site response because higher matric suction can significantly influence the dynamic soil properties. Further, NMRH04 is a soft soil site, categorized by NEHRP site class E (FEMA, 2009), where seismic site response may be significant. In addition, the depth of water table was estimated to be at 8 m for this site, which was relatively deep compared to other KiK-net sites. This groundwater depth may result in higher matric suction values (considering a linear suction profile) and intensify the effect of water table fluctuations on site response. The site consists of a 185-m layer of Quaternary soil (interbedded sand and sandy gravel) over layers of sandstone and siltstone. The profiles of shear and compression wave velocities are illustrated in Figure 1b, theoretical and empirical amplification spectra are illustrated in Figure 1c, and selected information on the monitored site is listed Table 1.

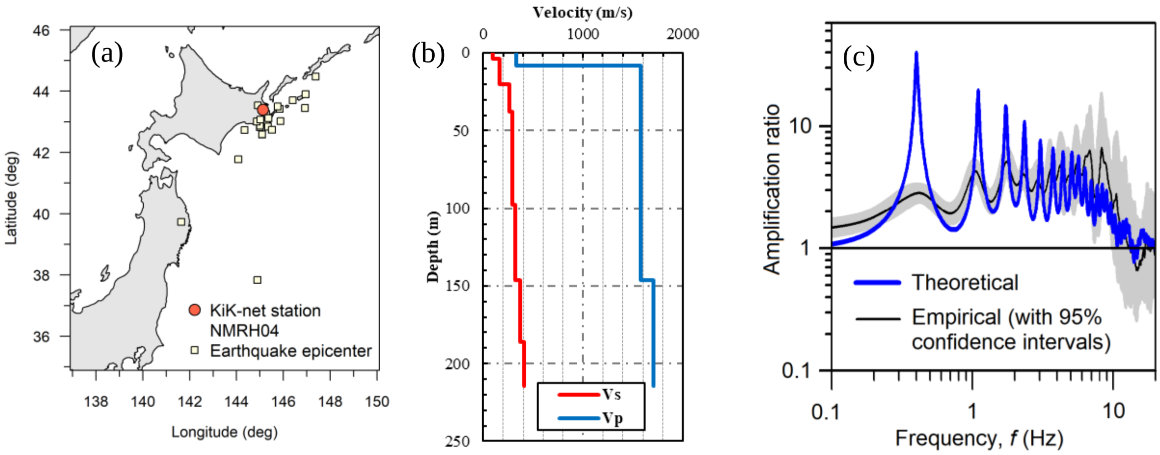

Figure 1. NMRH04: (a) Site location and epicenters of earthquakes used in the analyses, (b) shear and compression wave velocity profiles (NIED 2012), and (c) theoretical and empirical linear amplification spectra, along with 95% confidence intervals for the median empirical amplification spectra.

Table 1. Selected information on KiK-net station NMRH04 used in this study (NIED 2012)

Parameter	Value
Latitude (deg)	43.3953
Longitude (deg)	145.1264
Avg. shear-wave velocity over the top 30 m, $\bar{V}_{s,30}$ (m/s)	168
NEHRP site class	E
Depth to bedrock (m)	185
Depth of downhole seismometer (m)	216
Fundamental site frequency (Hz)	0.40
Geologic age of soil	Quaternary

2.2 *Equivalent Linear Site Response Models*

Equivalent-linear analyses were conducted in this study, as they lead to reasonable estimates of site response for PGA_{base} less than 0.2g (Assimaki et al. 2008) or strain levels less than 0.1% to 0.4% (Kaklamanos et al. 2013, Kim and Hashash 2013). The empirical equations of Boore (2016) were used to estimate the unit weight of soil layers based on the measured profiles of shear and compression wave velocities. The modulus reduction and damping curves were developed using the empirical framework proposed by Zhang et al. (2005). The modulus reduction curve (G/G_0), a function of shear strain γ, is computed as follows:

$$\frac{G}{G_0} = \frac{1}{\left(1 + \frac{\gamma}{\gamma_r}\right)^a} \tag{1}$$

$$\gamma_r = \gamma_{r1} \cdot \left(\frac{\sigma'_m}{P_a}\right)^k \tag{2}$$

where γ_r is the reference strain, a is the power index, γ_{r1} is the reference shear strain at a mean effective confining stress of 100 kPa, σ'_m is the mean effective confining stress, P_a is a reference stress of 100 kPa, and k is the stress correction factor. The values of γ_{r1}, k, and a are correlated with the Plasticity Index (PI) and the geologic age of soil deposits. Zhang et al. (2005) formulated an expression for the damping ratio (D) as a function of G/G_0:

$$D = 10.6\left(\frac{G}{G_0}\right)^2 - 31.6\left(\frac{G}{G_0}\right) + 21 + D_{min} \tag{3}$$

$$D_{min} = D_{min1}\left(\frac{\sigma'_m}{P_a}\right)^{-k/2} \tag{4}$$

$$D_{min1} = 0.008(\mathrm{PI}) + 0.82 \tag{5}$$

where D_{min} is the small-strain damping ratio, and D_{min1} is the small-strain damping ratio at a reference stress of 100 kPa. The selected dynamic formulations require the mean effective stress, PI, and geologic age of soil deposits as their inputs. Herein, the PI of the sand layer was assumed to be zero, and the geologic age of the deposit was obtained from the descriptions provided in the observation logs as Quaternary (Table 1). Since saturated layers are known to have compression wave velocities of 1000 to 2000 m/s (Haeni 1986, Grelle and Guadagno 2009), the depth of water table was estimated as the corresponding depth where the compression wave velocity reached 1500 m/s. The effective stress in the partially saturated zone was calculated considering the suction stress equation proposed by Lu et al. (2010):

$$\sigma' = (\sigma - u_a) + \sigma^s, \tag{6}$$

$$\sigma^s = \frac{S - S_r}{1 - S_r}(u_a - u_w) = \frac{u_a - u_w}{\left(1 + [\alpha\,(u_a - u_w)]^n\right)^{1-\frac{1}{n}}} \tag{7}$$

where σ^s is the suction stress; u_a and u_w are the pore air and pore water pressures, respectively; S is the degree of saturation; S_r is the residual degree of saturation; and α and n are the parameters for the van Genuchten soil-water retention curve (SWRC) model (van Genuchten 1980), respectively. In the absence of hydromechanical laboratory testing on the earthen materials, hydraulic properties of a typical fine well-graded sand (i.e. $\alpha = 0.1$, $N = 5$, and $S_r = 0.25$) were considered for ground layers in numerical models. It should be noted that the input parameters for soil profiles with the fluctuating water table were assessed using the values of the baseline model and the assumed SWRCs of the materials. Hydrostatic matric suction variations with no precipitation/evaporation were assumed when calculating the values of matric suction and degree of saturation above the water table.

2.3 *Incorporating Water Table Fluctuation in Site Response Analyses*

From the baseline level of 8 m, the water table level at NMRH04 was altered to two extreme levels, i.e. at the surface (0 m) and at 16 m below the ground surface, resulting in differences in shear wave velocity, unit weight, shear modulus-reduction curves, and damping curves (Figure 2). Variations of each parameter, aligned with the fluctuation of the water table, were determined using the baseline values in the soil profile. The variation of the moisture content ω versus depth was estimated using the fundamental relationship ω = S·e/G_s, where *S* is the degree of saturation, *e* is the void ratio (assumed to be 0.65; a typical value for loose sand), and G_s is the specific gravity (assumed to be 2.65). The values of degree of saturation at each depth were derived from the approximated SWRC. Given the values of moisture content at different depths and unit weight of the baseline soil profile at each level, the total unit weights versus depth could be inferred using the following equations:

$$\gamma_t = \gamma_d(1+\omega) \tag{8}$$

$$\frac{\gamma_{t1}}{\gamma_{t2}} = \frac{(1+\omega_1)}{(1+\omega_2)} \tag{9}$$

where γ_t is the total unit weight of the moist soil, γ_d is the dry unit weight, and ω is the moisture content. Subscripts denoted "1" refer to the revised values, and subscripts denoted "2" refer to the baseline values. The unified equation for estimating small-strain shear modulus in dry, unsaturated, and saturated conditions, proposed by Dong et al. (2016), was employed to estimate the divergence of shear modulus G_0 from those of the baseline soil layer:

$$G_0 = G_0^{Sat}\left(\frac{1}{S_e}\right)^{9.6.n^{-6}}\left(\frac{\sigma'}{P_{atm}}+1\right)^{\gamma_0} \tag{10}$$

where G_0^{sat} is the small-strain shear modulus of saturated soil without confinement, S_e is the effective degree of saturation, *n* is the van Genuchten fitting parameter, σ' is the mean effective stress, P_{atm} is the reference stress equal to atmospheric pressure, and γ_0 is an empirical fitting parameter (assumed to be 0.5 in this study). Since the value of G_0^{sat} is constant for soils with different degrees of saturation, the small-strain shear modulus for soil layers with fluctuating water table was obtained with respect to the baseline values, as follows:

$$\frac{G_{01}}{G_{02}} = \left(\frac{S_{e2}}{S_{e1}}\right)^{9.6n^{-6}}\left[\frac{\left(\frac{\sigma'_1}{P_{atm}}+1\right)}{\left(\frac{\sigma'_2}{P_{atm}}+1\right)}\right]^{\gamma_0} \tag{11}$$

where subscripts denoted "1" refer to the revised values, and subscripts denoted "2" refer to the baseline values. The shear-wave velocity V_S is then determined from the shear modulus G_0 using the physical relationship $V_S = [G_o/(\gamma_t/g)]^{1/2}$, where g = gravitational acceleration. Shear modulus reduction and damping curves were obtained using Equations 1 to 5, as a function of effective stress within the soil layers. The effective stress in different soil layers was estimated by adding the suction stresses caused by partial saturation, which varied depending on the water table level. The effect of water table fluctuation on V_s, G/G_0, and *D* is illustrated in Figure 2.

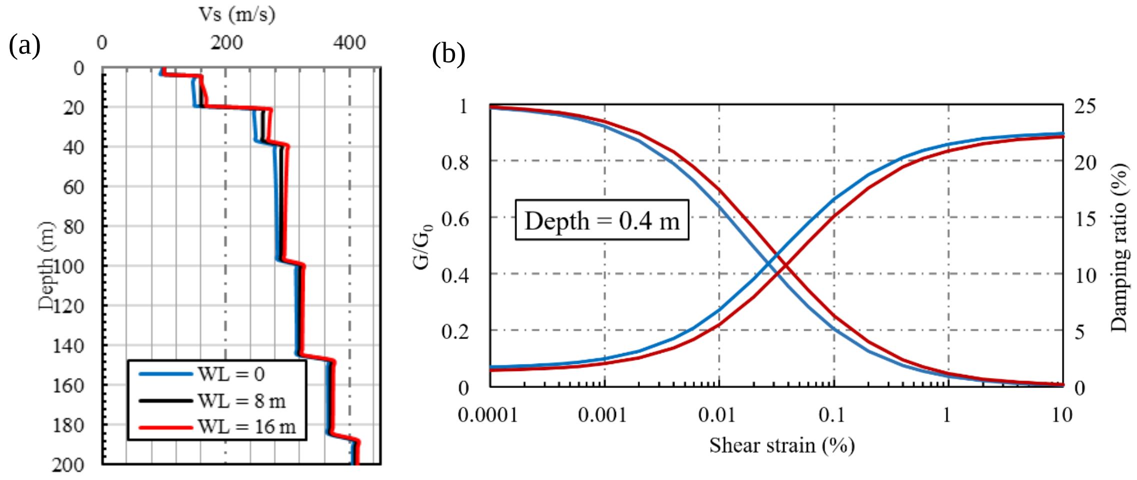

Figure 2. Effects of groundwater table fluctuation on (a) shear wave velocity and (b) shear modulus reduction factor and damping ratio at 0.4 m below the ground surface (similar values are observed for water level [WL] = 8 m and WL = 16 m).

2.4 *Input Motion Characteristics*

From the KiK-net database, we selected the acceleration time series of 23 seismic events measured at NMRH04, recorded at the ground surface and bedrock level, in both the North-South (NS) and East-West (EW) directions. The input motion illustrated in this study, recorded during a M_w 6.5 earthquake on 2000/12/22, has a $PGA_{bedrock}$ of 0.018g and $PGA_{surface}$ of 0.0946g. Its pseudo-spectral acceleration in the NS and EW directions are illustrated in Figure 3a and 3b, respectively. The selected motion encompasses a wide range of frequencies, allowing for the effect of partial saturation or water table fluctuation to be observed for different frequency ranges.

3 VERIFICATION OF NUMERICAL MODELING

The numerical analysis in this study was verified against an EL analysis, using SHAKE2000 (Ordonez 2000), as well as a nonlinear (NL) analysis using DEEPSOIL (Hashash et al. 2016) for the same site, as reported by Kaklamanos et al. (2015). Similar to conventional site response procedures, the soil above the water table was assumed to be completely dry, and the effect of partial saturation was not considered in this step. The resulting pseudo-spectral accelerations (PSA) were plotted against those recorded by the accelerograms at the ground surface (observed motions) as well as the results of Kaklamanos et al. (2015), as shown in Figure 3.

Although the equivalent linear analysis in Kaklamanos et al. (2015) was performed using a different program, both equivalent linear models, in SHAKE and DEEPSOIL, led to very similar spectral acceleration values at the surface, as expected. This is attributed to similarities in the soil profiles, soil properties, and analysis types. Although the observed values are different from those obtained numerically, especially for the NS motion, this variance is a result of a number of uncertainties in site response analysis including the estimated soil properties, modeling a 3D motion using a simplified 1D analysis, and potentially the depth of groundwater table at the time of the seismic event. Overall, the observed trends validate the procedure of the numerical modeling in this study.

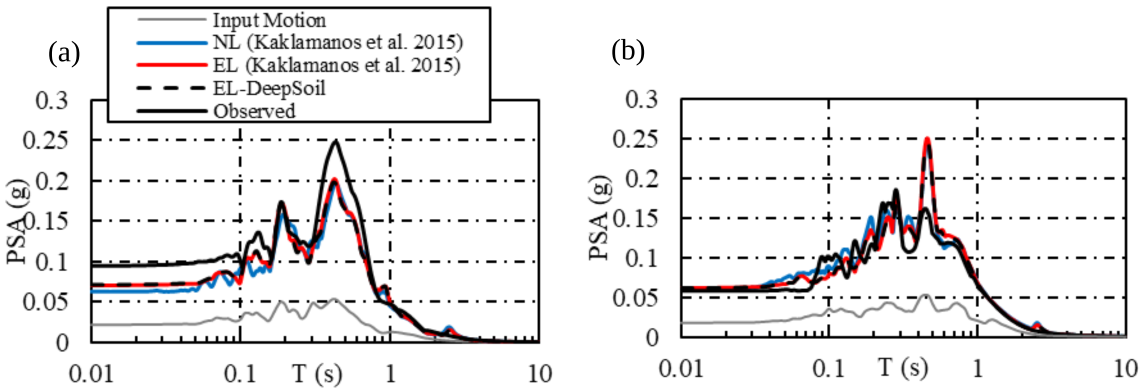

Figure 3. Verification of numerical models for pseudo-spectral acceleration against observed ground motions and other numerical analyses (Kaklamanos et al. 2015) for (a) NS motion and (b) EW motion.

4 RESULTS AND DISCUSSION

In order to understand the sensitivity of analyses to the change in each parameter, a number of models were analyzed in which only one parameter (i.e. G_0, D, G/G_0, or γ) was changed at a time (Mirshekari 2018). Ultimately, a set of analyses were performed with all the input parameters changed simultaneously as a result of groundwater fluctuation. The results of these analyses manifest the total influence of water table fluctuation on ground-surface motion characteristics. The surface motion for each analysis was calculated as the geometric mean of EW and NS ground motions. This geometric mean was then post-processed to obtain different motion characteristics, including surface-to-base ratio of response spectra (RRS) as well as surface-to-base FFT transfer functions (TF). The results in terms of RRS are illustrated in Figure 4a. To visually illustrate the range of variations in RRS when only one parameter was altered, those results are also shown in Figure 4 with gray dashed lines. For a detailed parametric evaluation on the seismic response of sites with different groundwater levels, please refer to Mirshekari (2018). To evaluate the divergence of each parameter from the observed RRS, the residuals were computed using Equation 12 and are plotted in Figure 4b:

$$RRS_{Residual} = ln(RRS_{Observed}) - ln(RRS_{Predicted}) \tag{12}$$

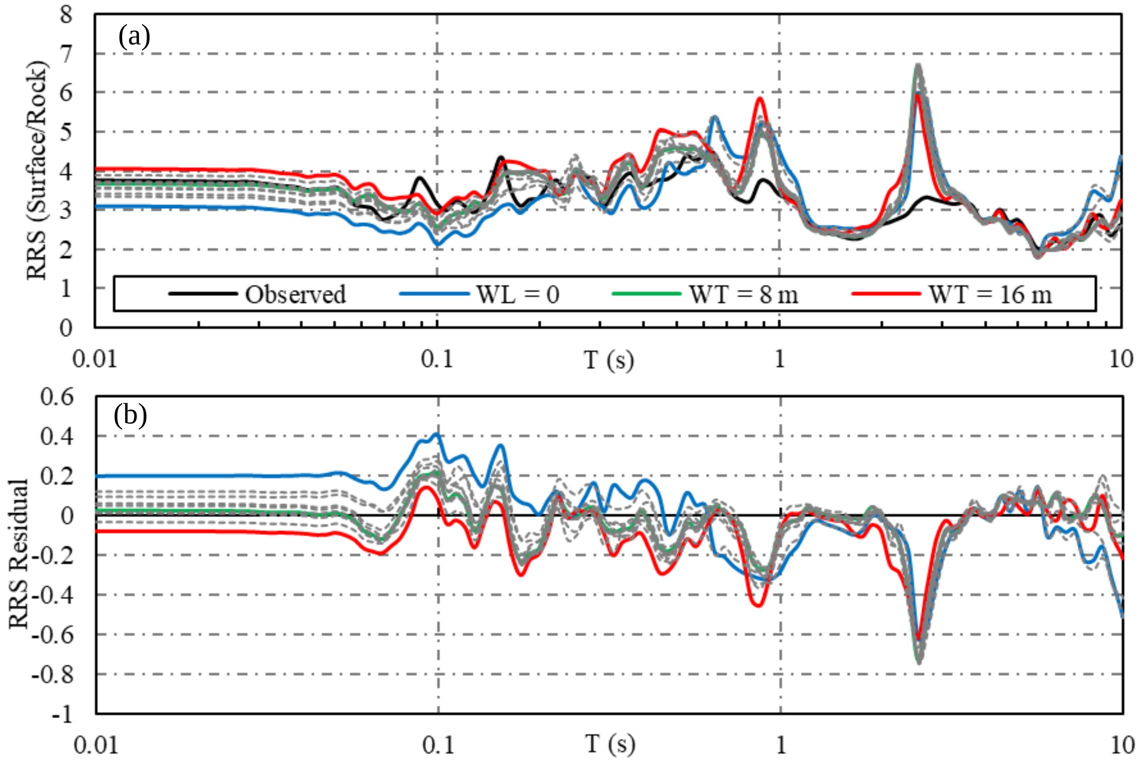

Figure 4. (a) Surface-to-rock ratio of response spectra and (b) Surface-to-base RRS residual for soil profiles with different water table levels. The results of analyses with only one parameter changed for each water table level are shown with dashed lines.

Elevating the water table level to the ground surface led to significantly lower RRS values for periods less than approximately 0.5 s and slightly higher values for longer periods. The soil profiles with the water table at 16 m depth (i.e. stiffer ground) showed higher RRS values for almost all periods. This is contradictory to the assumption of smaller amplification factors for soils with higher stiffness. These trends were observed due to interaction between the effects of variations in different input parameters. Similar trends of higher amplification factors in stiffer partially-saturated ground were previously observed numerically (Ghayoomi and Mirshekari 2014) and experimentally (Mirshekari and Ghayoomi 2017b, 2018). For the deeper water level, while the increase in shear modulus profile led to lower RRS, the counter-effects caused by lower damping and unit weight profiles led to an overall increase in terms of RRS comparing with the baseline curves. Furthermore, the results show that water table fluctuation leads to a significant variation in terms of RRS for different period ranges, inducing a high level of uncertainty in SSRA that has to be considered when using the results for design purposes. The strongest deviations were observed at short spectral periods, whereas the predictions were relatively similar (all consistent in overprediction) in the vicinity of the fundamental mode of vibration (at 2.5 s).

FFT transfer functions for ground layers with different water table levels are shown in Figure 5. The frequency range in Figure 5 was limited to 5 Hz to better illustrate the variations in the transfer functions. The transfer functions appear to be more sensitive to the variations in groundwater level than the ratios of response spectra. The fundamental frequencies increase as a result of lowering the water table and decrease due to elevating the water level, indicating stiffer and softer materials in each case, respectively. The differences were more substantial at the higher modes of vibration rather than at the fundamental mode. However, as discussed earlier, the stiffer material with the deeper water table had a higher amplification factor due to the interaction between different soil parameters. The acceleration amplification factor is inversely proportional to both stiffness and damping of a simplified single degree of freedom system (Roesset 1977). Lowering the groundwater level generates a stiffer medium which, in turn, translates into higher shear modulus and lower damping over depth. These variations in dynamic soil properties would have counter-effects on the ultimate amplification factor. Further, the decrease in the unit weight of layers with lower water levels was shown to lead to higher amplification factors. These alterations due to the change in each parameter collectively led to an ultimate increase in amplification factor due to lowering the groundwater level. An opposite trend would be observed when the water table is elevated.

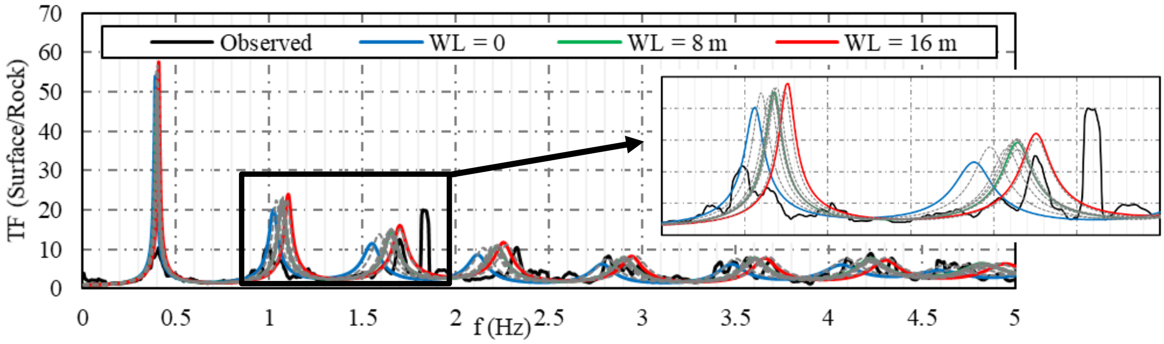

Figure 5. Surface-to-rock transfer functions for soil profiles with different water table levels. The results of analyses with only one parameter changed for each water table level are shown with dashed lines.

5 CONCLUSIONS

The results of a sensitivity analysis were presented on the effects of water table fluctuations on seismic site response at the NMRH04 site in the KiK-net database. The depth of the groundwater table was altered from 8 m below the ground surface to two extreme levels (at the surface and at 16 m depth). The alterations in groundwater level led to a significant change in both the RRS and the FFT transfer functions. A lower groundwater level translates into a stiffer soil profile with higher shear modulus, lower damping, and lower unit weight. The interaction between the effects caused by the variations in each of these parameters led to an increase in amplification factor due to lowering the water level. For softer ground layers with higher water levels, an opposite trend – a decrease in amplification – was observed.

REFERENCES

Adalier, K. & Elgamal, A. W. 2001. Seismic Response of Dense and Loose Sand Columns. *Intl. Conferences on Recenet Advances in Geotechnical Earthquake Engineering and Soil Dynamics*, 14, 1-6.

Aoi S, Obara K, Hori S, Kasahara K & Okada Y. 2000. New Japanese uphole-downhole strong-motion observation network: KiK-net. *Seismological Research Letters*; 72:239.

Assimaki, D., Li, W., Steidl, J. & Schmedes, J. 2008. Quantifying nonlinearity susceptibility via site-response modeling uncertainty at three sites in the Los Angeles Basin. *Bulletin of the Seismological Society of America*, 98(5), 2364-2390.

Boore, D. M. 2016. Determining Generic Velocity and Density Models for Crustal Amplification Calculations, with an Update of the Generic Site Amplification for Vs = 760 m/s. *Bulletin of the Seismological Society of America*, 106(1), 313-317.

Boore, D. M., Joyner, W. B. & Fumal T. E. 1994. Estimation of Response Spectra and Peak Accelerations from Western North American Earthquakes: An Interim Report, Part 2. *USGS*, 94-127, 40 pp.

D'Onza, F., d'Onofrio, A. & Mancuso, C. 2008. Effects of unsaturated soil state on the local seismic re-

sponse of soil deposits. *Proc. 1st European Conf. on Unsaturated Soils*, Durham, UK, 531- 536.
Federal Emergency Management Agency, FEMA. 2009. NEHRP Recommended Seismic Provisions for New Buildings and Other Structures. *FEMA* P-750.
Ghayoomi, M. & Mirshekari, M. 2014. Equivalent Linear Site Response Analysis of Partially Saturated Sand Layers. *UNSAT2014 conference*, Sydney, Australia, 1-6.
Ghayoomi, M., Suprunenko, G. & Mirshekari, M. 2017. Cyclic Triaxial Test to Measure Strain-Dependent Shear Modulus of Unsaturated Sand. *ASCE Intl. Journal of Geomechanics*, 17(9), 1-11.
Gheibi, A., & Hedayat, A. 2018. Ultrasonic investigation of granular materials subjected to compression and crushing. *Ultrasonics*, 87, 112-125.
Grelle, G. & Guadagno, F. M. 2009. Seismic refraction methodology for groundwater level determination: Water seismic index. *Journal of Applied geophysics*, 68(3), 301-320.
Haeni, F. P. 1986. Application of seismic refraction methods in groundwater modeling studies in New England. *Geophysics*, 51(2), 236-249.
Hashash, Y.M.A., Musgrove, M.I., Harmon, J.A., Groholski, D.R., Phillips, C.A. & Park, D. 2016. DEEPSOIL 6.1, User Manual. *Urbana, IL, University of Illinois at Urbana-Champaign*.
Hoyos, L.R., Suescun-Florez, E.A. & Puppala, A.J. 2015. Stiffness of Intermediate Unsaturated Soil from Simultaneous Suction-Controlled Resonant Column and bender Element Testing. *Engineering Geology*,188, 10-28.
Jarast, P., & Ghayoomi, M. 2017. Numerical Modeling of Cone Penetration Test in Unsaturated Sand Inside a Calibration Chamber. *International Journal of Geomechanics*, 18(2), 04017148.
Kaklamanos, J., Bradley, B. A., Thompson, E. M. & Baise, L. G. 2013. Critical parameters affecting bias and variability in site response analyses using KiK-net downhole array data. *Bulletin of the Seismological Society of America*, 103 (3): 1733-1749.
Kaklamanos, J., Baise, L. G., Thompson, E. M. & Dorfmann, L. 2015. Comparison of 1D Linear, Equivalent-linear, and Nonlinear Site Response Models at Six KiK-net Validation Sites. *Soil Dynamics and Earthquake Engineering*, 69, 207-219.
Kaklamanos, J. & Bradley, B.A. 2018. Challenges in predicting seismic site response with 1D analyses: Conclusions from 114 KiK-net vertical seismometer arrays. *Bulletin of the Seismological Society of America*, 108 (5A): 2816-2838.
Kim, B. & Hashash, Y. M. 2013. Site response analysis using downhole array recordings during the March 2011 Tohoku-Oki earthquake and the effect of long-duration ground motions. *Earthquake Spectra*, 29 (s1), S37-S54.
Lu, N., Godt, J. W. & Wu, D. T. 2010. A Closed Form Equation for Effective Stress in Unsaturated Soil. *Water Resources Research*, 46, W05515, 14pp.
Mancuso, C., Vassallo, R. & d’Onofrio. A. 2002. Small strain behavior of a silty sand in controlled-suction resonant column – torsional shear tests. *Canadian Geotechnical Journal*, 39, No. 1, 22–31.
Mirshekari, M. & Ghayoomi, M. 2015. Simplified Equivalent Linear and Nonlinear Site Response Analysis of Partially Saturated Soil Layers. *IFCEE 2015, Geotechnical Special Publication 256, M. Iskander, M.T. Suleiman, J.B. Anderson, D.F. Laefer eds.*, San Antonio, Texas, 2131-2140.
Mirshekari, M. 2018. Seismic Site Response of Partially Saturated Soil Layers. *Ph.D. Dissertation, University of New Hampshire*, Durham, NH.
Mirshekari, M. & Ghayoomi, M. 2017a. Simulating Seismic Response of Unsaturated Sand Layers inside a Geotechnical Centrifuge. *19th International Conference on Soil Mechanics and Geotechnical Engineering*, Seoul, South Korea: 1-4.
Mirshekari, M. & Ghayoomi, M. 2017b. Centrifuge Tests to Assess Seismic Site Response of Partially Saturated Sand Layers. *Soil Dynamics and Earthquake Engineering*, Vol. 94, pp. 254-265.
Mirshekari, M. & Ghayoomi, M. 2018. Effects of shaking intensity on seismic response of unsaturated sand layers. *In Proc. of the 7th International Conference on Unsaturated Soils*.
Mousavi, S. & Ghayoomi, M. 2018. Dynamic shear modulus of microbial induced partially saturated sand. *IS Atlanta – B2G Atlanta 2018*, Atlanta, GA, 6 pp.
National Research Institute for Earth Science and Disaster Prevention (NIED) 2012. In: Strong-motion seismograph networks (KiK-net), *available at http://www.kyoshin.bosai.go.jp/*; (accessed in 2018).
Ordóñez GA. 2010. SHAKE2000: a computer program for the 1-D analysis of geotechnical earthquake engineering problems (User's Manual). *Lacey, Washington: GeoMotions, LLC*; (262 pp).
Stewart, J.P., Liu, A.H. & Choi, Y. 2003. Amplification Factors for Spectral Acceleration in Tectonically Active Regions. *Bull. Seism. Soc. Am.*, 93 (1), 332-352.
Thompson, E.M., Baise, L.G., Tanaka, Y. & Kayen, R.E. 2012. A taxonomy of site response complexity. *Soil Dynamics and Earthquake Engineering* 41: 32-43.
van Genuchten, M. 1980. A Closed Form Equation for Predicting the Hydraulic Conductivity of Unsaturated Soils. *Soil Sci. Soc. Am. J.*, Vol. 58, pp. 647–652.
Zhang J, Andrus R. D. & Juang, C. H. 2005. Normalized Shear Modulus and Material Damping Relationships. *Journal of Geotechnical and Geoenvironmental Engineering*, 131 (453-464).